



Cite this: DOI: 10.1039/d5fb00734h

Enhanced techno-functional and bioactive characteristics of dietary fibre from banana pseudostem scutcher through greener technologies

Paramasivam Suresh Kumar * and Magesh Kumar Birundha

Dietary fibre (DF), an essential nutrient for digestive and metabolic health, is gaining global traction due to its role in preventing lifestyle disorders and its incorporation into functional and sustainable food systems. This study examined the impact of different extraction techniques, namely chemical (CHE), hot water (HWE), microwave-assisted (MAE), ultrasound-assisted (UAE), and dual (UAE + MAE), on the yield and functional properties of dietary fibre (DF) derived from banana pseudostem scutcher. The true extraction yield of DF ranged from $50.54 \pm 2.38\%$ (HWE) to $81.67 \pm 0.15\%$ (UAE + MAE). The total dietary fibre (TDF) content was highest in UAE + MAE samples, showing nearly 35% higher TDF and 40% higher SDF than HWE, while insoluble dietary fibre (IDF) increased by 30% under UAE. Functionally, UAE + MAE-treated fibres exhibited superior water-holding capacity (6.42 g g^{-1}), oil-holding capacity (4.98 g g^{-1}), and swelling power (5.75 g g^{-1}), indicating 1.8–2.0-fold improvements over CHE method. These enhancements were attributed to increased hydrogen bond exposure, changes in morphology and structure, as confirmed by SEM and FTIR, while XRD revealed reduced crystallinity and increased amorphous regions. The same treatment also improved glucose (81.2 mmol g^{-1}), cholesterol (3.2-fold), and nitrite ion (32.8 mg g^{-1}) adsorption capacities. In summary, ultrasound and dual ultrasound–microwave treatments effectively enhanced yield and techno-functional quality, demonstrating the potential of banana scutcher as a sustainable, high-value dietary fibre source for functional food and nutraceutical industries.

Received 25th October 2025

Accepted 26th March 2026

DOI: 10.1039/d5fb00734h

rsc.li/susfoodtech

Sustainability spotlight

The integration of non-thermal, green extraction techniques, such as the combined ultrasound- and microwave-assisted (UAE + MAE) process, offers a sustainable pathway for valorizing banana pseudostem scutcher. This approach minimizes chemical waste while preserving nutritional and functional qualities, supporting SDG 3 (Good Health and Well-being) through the promotion of disease-preventive diets and SDG 9 (Industry, Innovation, and Infrastructure) by advancing clean and innovative processing technologies. The study highlights the potential of high-value dietary fibre recovery within circular bioresource frameworks, demonstrating a strategic route toward sustainable food system transitions.

1 Introduction

The growing awareness about diet and health has resulted in a surge in the development of functional foods and nutraceuticals. Modern dietary patterns have led to an increase in lifestyle-related diseases such as hypertension,¹ obesity,² cardiovascular diseases³ and diabetes.⁴ This has driven a growing demand for dietary fibre-rich food products to combat these health challenges. The global dietary fibre market, valued at 7.9 billion USD in 2023, is expected to expand

to 14.93 billion USD by 2030, registering a compound annual growth rate (CAGR) of 9.5%⁵ between 2024 and 2030. Dietary fibre (DF) refers to a carbohydrate polymer derived from plants that is resistant to enzymatic hydrolysis in the small intestine of humans.⁴ This has been increasingly recognised for its function and health-promoting properties. It is the seventh fundamental nutrient required for the human body.⁶ Dietary fibre is categorised into two types based on their solubility: soluble dietary fibre (SDF) and insoluble dietary fibre (IDF), where SDF includes hemicellulose, gums, mucilage and pectin.⁷ It is highly valued for its capacity to retain water, ability to bind bioactive molecules and interfacial properties.^{8,9} In contrast, IDF is composed of lignin, cellulose, and insoluble hemicellulose. The fibre fermentation in the colon produces short chain fatty acids including butyrate, which reduces the risk of colon cancer.¹⁰ It

Division of Crop Production and Post-Harvest Technology, ICAR-National Research Centre for Banana, Thogamalai Road, Thayanur Post, Tiruchirappalli, Tamil Nadu 620 102, India. E-mail: psureshars@gmail.com; Fax: +91-4312618125; Tel: +91-9626257154



stimulates bowel movement by bulking stool and aiding faecal elimination.¹¹ It is less fermentable than SDF and is pivotal in maintaining digestive health and accelerating gastrointestinal transit time. The functional properties of both SDF and IDF are profoundly linked to their matrix structure, particle size and methods used for their extraction.¹² Processing conditions such as temperature, pH and mechanical disruption can greatly impact their physicochemical behaviour.¹³ DF is commonly incorporated in bakery products such as breakfast cereals, muffins, and bread to enhance their texture, water and oil retention capacity, nutritional value and shelf life.¹⁴ Beverages such as juices, smoothies and nutritional supplement drinks are often fortified with DF to stabilise suspensions and improve mouthfeel.¹³

The most commonly used sources for dietary fibre extraction are cereal brans (mainly wheat and oats), sugar beet pulp, and fruit pomaces such as apple and citrus. Over the decade, much research has been carried out to extract DF from various sources, such as orange peel,¹⁵ passion fruit,¹⁶ grape peel,⁸ kiwi, rice bran,¹⁷ and flaxseed.¹⁸ Orange peel (67.27–76.69%), passion fruit peel (62.64%) and kiwi fruit (92.88%) yielded different levels of DF depending on the extraction methods. Considering the demand, new sources are being explored for the extraction of dietary fibre. In that context, globally, around 300–350 million metric tons (fwb) of banana biomass including pseudostem, leaves, bloom (bell), and corm are discarded annually after harvesting the bunches. Among these, scutcher biomass generated after fibre extraction from the pseudostem accounts for nearly 30–35% of the total plant weight, equating to approximately 7–10 tons per hectare on a dry weight basis. This lignocellulosic residue is typically disposed of, leading to the release of greenhouse gases such as carbon dioxide, methane and nitrous oxide.

Conventionally, DF extraction is carried out using alkali (NaOH) at the industrial level. This approach often alters the structural integrity, diminishing its nutritional properties, and also causes secondary environmental pollution.⁷ In this method, chemicals are used to break the cross-linkages of water-soluble polysaccharides and ester bonds. In contrast, hot water extraction offers a more sustainable method but results in a lower yield of true dietary fibre with more impurities.⁸ Enzymatic extraction using protease, α -amylase, and amyloglucosidase is time-consuming, costly, and requires stringent pH and temperature control.²⁰ In response to the limitations of different methods, researchers began exploring milder and environmentally friendly alternatives such as ultrasound- and microwave-assisted extractions to improve efficiency, enhance nutritional functionalities and reduce environmental impact.^{8,21} Microwave extraction and dielectric heating are being used to rupture the cell walls, while ultrasound extraction exploits acoustic cavitation to enhance penetration and disrupt fibre matrices.^{22–27}

Although ultrasound- and microwave-assisted extraction techniques have been widely applied to enhance dietary fibre recovery from agro-industrial residues,^{15–19} studies on banana-derived materials have largely focused on peel,⁹ with no reports on banana scutcher. This highlights a clear research gap

in the valorisation of this underutilised lignocellulosic residue. The novelty of this study lies in the first exploration of banana scutcher as a dietary fibre source using ultrasound, microwave, and their combined pre-treatment strategies to enhance fibre yield and functionality. It is thus hypothesised that scutcher, an underutilised lignocellulosic residue of banana pseudostem, when subjected to targeted pre-processing modifications, could yield dietary fibre with enhanced techno-functional and bioactive characteristics. Accordingly, this study aims to evaluate the effects of these treatments on dietary fibre yield, composition, and techno-functional properties and identify the most effective extraction approach.

2 Materials and methods

2.1 Materials and chemicals

Banana pseudostem scutcher from var. Grand Naine (AAA genome) was collected after the extraction of fibre, fed into a hydraulic press to drain the excess sap water, washed thoroughly, and dried in a hot air oven (Universal NSW-143 (OSS-7), Delhi, India) at 60 °C for 48 h. It was then ground using a mixer (Model: Bosch MGM8642BIN/01, Mumbai, India), sieved through a 60 mesh (250 μ m sieve) and stored in zip-lock HDPE pouches. The total dietary fibre kit (TDF100A-1 KT) containing α -amylase, protease and amyloglucosidase was obtained from Sigma Aldrich (St Louis, MO, USA). All other chemicals used in the study were of analytical grade and were purchased from Hi Media, Mumbai, India.

2.2 Extraction of dietary fibre

2.2.1 Chemical extraction. The alkali method (CHE) of extraction of DF was carried out using 2% (w/v) NaOH, according to the method reported by Wang *et al.*,²⁴ with minor modifications. Briefly, 50 g of scutcher was suspended in 1000 mL NaOH solution and kept at 80 °C in a water bath for 2 h, followed by centrifugation at 6000 rpm for 10 min. Later, the residue was rinsed thrice with distilled water and dried in a hot air oven at 60 °C. The dried sample was then ground using a mixer, sieved through a 60 mesh (250 μ m) sieve and packed in a HDPE pouch for further use.

2.2.2 Hot water extraction (HWE). The hot water extraction of dietary fibre from banana scutcher was carried out following the method of Kaur *et al.*,²⁵ with subtle alterations. Briefly, 50 g of sample was taken, and 1000 mL of distilled water was added (1 : 20 ratio) and placed in a water bath at 95 °C for 120 min, followed by centrifugation at 6000 rpm for 10 min. Then, the sample was processed as per the process outlined in Section 2.2.1.

2.2.3 Microwave-assisted extraction (MAE). DF from banana scutcher was extracted according to the method of Wen *et al.*²⁸ with slight modifications. Precisely, 50 g of sample was mixed with distilled water at a 1 : 20 (w/v) ratio. The suspension was irradiated at 900 W for 5 min in a microwave oven (IFB, 30FRC2, China) and centrifuged at 6000 rpm for 10 min. Then, the sample was processed as per the process outlined in Section 2.2.1.



2.2.4 Ultrasound-assisted extraction (UAE). For ultrasound-assisted extraction (UAE), the sample was processed according to Rawat *et al.*,²⁹ Briefly, the prepared sample was sonicated for 60 min at 70% amplitude using a probe ultrasonicator (150 W, 20 kHz; Model VCX 130, Sonics & Materials Inc., USA) equipped with a 13 mm diameter titanium probe immersed 30 mm into the solution. Sonication was carried out in pulse mode (10 s on, 20 s off), followed by centrifugation at 6000 rpm for 10 min. Then, the sample was processed as per the process outlined in Section 2.2.1.

2.2.5 Dual extraction. In dual extraction, the sample was first subjected to UAE to enhance cell disruption and improve microwave penetration efficiency under the conditions described in Section 2.2.4, followed by MAE treatment according to Section 2.2.3. After each extraction process, the treated samples were further processed according to the procedure described in Section 2.2.1.

2.3 Physicochemical characterisation of DF

2.3.1 Proximate composition. The obtained dietary fibre samples *via* different treatments were subjected to proximate analysis, including moisture (AOAC 925.10), ash (AOAC 923.03), crude protein (AOAC 979.09; Kjeldahl method with a nitrogen-to-protein conversion factor of 6.25), and crude fat (AOAC 920.39; Soxhlet extraction), following standard methods of the Association of Official Analytical Chemists³⁰ (AOAC, 2019). The water activity of the samples was also measured. Total carbohydrate content was calculated by difference using the formula: carbohydrates (%) = 100 – (moisture + crude protein + crude fat + ash).

The dietary fibre extraction yield of various treatments was calculated using the following formula:^{26,27}

$$\text{True dietary fibre yield(\%)} = \frac{\text{final biomass yield} \times \text{TDF}}{100} \quad (1)$$

2.3.2 Estimation of dietary fibre. Total dietary fibre (TDF), soluble dietary fibre (SDF), and insoluble dietary fibre (IDF) contents were determined using the enzymatic–gravimetric method according to AOAC Official Method 991.43 (AOAC, 2002), with slight modifications. Briefly, samples were gelatinised with heat-stable α -amylase at 95 °C for 15 min to hydrolyse starch, followed by protease treatment at 60 °C for 30 min to remove protein and subsequent incubation with amyloglucosidase at 60 °C for 30 min to ensure complete starch hydrolysis. After enzymatic digestion, the mixture was filtered to separate the insoluble dietary fibre (IDF) fraction. The filtrate was then treated with 95% ethanol (1 : 4, v/v) and allowed to stand overnight at room temperature (27 ± 2 °C) to precipitate soluble dietary fibre (SDF). The precipitate was recovered by filtration, washed sequentially with ethanol and acetone, and dried at 50 °C for 24 h. Both IDF and SDF residues were corrected for protein and ash contents, and TDF was calculated as the sum of IDF and SDF.²⁷

2.3.3 Color. The CIE L^* , a^* , and b^* colour parameters of the dietary fibre were measured using a hand-held chroma meter

(CR-400, Minolta Co., Ltd, Japan). The instrument was calibrated using a white standard under CIE standard illuminant D65, and measurements were performed using a 45°/0° geometry.²⁷

2.3.4 Flow characteristics. The bulk density of the dietary fibre was measured as the ratio of the sample's mass to the volume it occupied. The tapped density was determined by repeatedly tapping the measuring cylinder over 100 times and calculating the ratio of the sample's weight to its tapped volume. To calculate the Carr Index (CI) and Hausner Ratio (HR), the following equations were used^{26,27}

$$\text{CI(\%)} = \frac{\text{tapped density} - \text{bulk density}}{\text{tapped density}} \times 100 \quad (2)$$

$$\text{HR} = \frac{\text{tapped density}}{\text{bulk density}} \quad (3)$$

2.4 Secondary metabolites

Total phenolic content (TPC) was determined using a modified Folin–Ciocalteu method. Briefly, an aliquot of the sample extract was reacted with Folin–Ciocalteu reagent followed by sodium carbonate, and the absorbance was measured at 765 nm using a UV-Vis spectrophotometer. TPC was quantified using a gallic acid calibration curve and expressed as milligrams of gallic acid equivalents (mg GAE/100 g) of sample. Total flavonoid content (TFC) was determined using the aluminium chloride colorimetric method. The reaction mixture was incubated, and absorbance was measured at 415 nm. TFC was calculated using a quercetin standard calibration curve and expressed as milligrams of quercetin equivalents (mg QE/100 g) on a dry weight basis. Antioxidant activity was evaluated using the DPPH (2,2-diphenyl-1-picrylhydrazyl) radical scavenging assay. The decrease in absorbance was recorded at 517 nm, and the results were expressed as percentage inhibition of the DPPH.³¹

$$\text{DPPH scavenging activity(\%)} = \frac{\text{absorbance of control} - \text{absorbance of sample}}{\text{absorbance of control}} \quad (4)$$

2.5 Techno-functional characterisation

2.5.1 Hydration properties and oil holding capacity. Water holding capacity (WHC) (5) and swelling property (SP) (6) were determined at 60 °C and oil holding capacity (OHC) (7) was also measured using our previously standardised procedures.^{27,31}

$$\text{WHC (g g}^{-1}\text{)} = \frac{W_f - W_i}{W_i} \quad (5)$$

$$\text{SP (mL g}^{-1}\text{)} = \frac{V_2 - V_1}{W_i} \quad (6)$$

$$\text{OHC (g g}^{-1}\text{)} = \frac{W_f - W_i}{W_i} \quad (7)$$



W_i is the initial weight of the sample, W_f is the final weight of the sample, and V_1 and V_2 are the volumes of the sample.

2.5.2 Emulsifying activity (EA). The emulsifying activity of the extracted dietary fibre was studied according to the method of Chinnathambi *et al.*, 2024³² with slight changes. Briefly, 5 mL of DF solution (0.5% w/v) was prepared, and 5 mL of refined sunflower oil was added to it. The sample solution was mixed using a homogeniser (ULTRA-TURRAX T 25 digital, IKA-Werke GmbH & Co. KG, Germany) at 2000 rpm for 3 min and then centrifuged at 6000 rpm for 10 min. The EA% was determined using the following formula:

$$\text{EA}(\%) = \frac{V_1}{V_2} \times 100 \quad (8)$$

V_1 is the volume of the emulsified layer and V_2 is the total volume of the solution.

2.6 Bioactive adsorption analysis

2.6.1 Glucose adsorption capacity (GAC). GAC was measured by the approach followed by Gan *et al.*, 2020³³ with slight modifications. Briefly, 0.5 g of the sample was added into glucose solutions at diverse concentrations (50, 100, 150, and 200 mmol L⁻¹) and incubated for 2 h at 37 °C. After incubation, the mixture was centrifuged at 3000 rpm for 20 min and 0.5 mL was collected in a glass tube. 3 mL of distilled water and 2 mL of dinitro-salicylate (DNS) were then added to it and mixed well. The mixture was incubated at 95 °C for 6 min with continuous agitation. After cooling to room temperature, the absorbance was measured at 540 nm. The GAC was calculated using the following formula:

$$\text{GAC} \left(\frac{\text{mmol}}{\text{g}} \right) = \frac{G_1 - G_2}{R_1} \times V \quad (9)$$

where G_1 is the glucose level in supernatant before adsorption, G_2 is the amount of glucose after adsorption, R_1 is the residue weight, and V is the volume of glucose solution.

2.6.2 Nitrite ion adsorption capacity (NIAC). The measurement of NIAC was determined by the method reported by Peng *et al.*,³⁴ with some modifications. The extracted dietary fibre sample of 0.5 g was mixed with 5 mL of NaNO₂ solution (20 µg mL⁻¹), and the pH was adjusted to 7.0 and 2.0 to stimulate the environment of the small intestine and stomach, respectively. The mixture was placed in a water bath at 37 °C for 2 h. After centrifugation at 5000 rpm for 15 min, 0.4 mL of the supernatant was transferred into a glass tube. 2 mL of distilled water was added. 2 mL of *p*-aminobenzenesulfonic acid (sulfanilic acid, 4 µg per mL) and 1 mL of *N*-(1-naphthyl)ethylenediamine dihydrochloride (2 µg per mL) were then added to the mixture. The solution was incubated for 30 min under dark conditions. The solution was measured at 538 nm using a spectrophotometer and the following equation was used for calculation:

$$\text{NIAC}(\mu\text{g g}^{-1}) = \frac{N_1 - N_2}{S_1} \times V \quad (10)$$

where N_1 is the concentration of NaNO₂ in the solution before adsorption, N_2 is the concentration of NaNO₂ after adsorption, and S_1 is the sample weight.

2.6.3 Cholesterol adsorption capacity (CAC). CAC was determined by the method of He *et al.*,³⁵ with some modifications. Egg yolk was mixed with distilled water at a 1 : 9 ratio and was whipped into an emulsion. 0.5 g of sample was weighed and 5 mL of emulsion was added to it and shaken at room temperature (27 °C ± 2) for 2 h, and then it was centrifuged at 4800 rpm for 10 min. Later, 1 mL of the supernatant was collected and diluted 10 times with glacial acetic acid, and 0.4 mL was taken to determine the cholesterol content. Egg yolk emulsion was used as a blank but without dietary fibre and CAC was calculated using the following formula:

$$\text{CAC}(\text{mg g}^{-1}) = \frac{M_1 - M_2}{M_0} \quad (11)$$

where M_1 is the weight of cholesterol in the solution before adsorption, M_2 is the amount of cholesterol after adsorption, and M_0 is the sample weight.

2.7 Morpho-structural analysis

2.7.1 Scanning electron microscopy. The external morphology of the modified flours was examined using a scanning electron microscope (VEGA3, TESCAN, Czech Republic) operated at an accelerating voltage of 5 kV. A small portion of the DF was mounted on aluminium SEM stubs with double-sided conductive adhesive tape, which secured the sample and provided electrical contact to minimize charging effects. To further enhance conductivity and image clarity, the samples were coated with a thin layer of gold using a sputter coater under vacuum conditions. This coating reduced surface charging and enabled high-resolution imaging for precise observation of the DF morphology.^{26,27}

2.7.2 Fourier transform infrared (FT-IR) spectroscopy. The functional groups of the dietary fibre samples were characterised using Fourier Transform Infrared (FTIR) spectroscopy. The dried dietary fibre was finely ground and homogenised with potassium bromide (KBr) powder to achieve uniform mixing. The mixture was compressed under high pressure to obtain transparent pellets suitable for infrared analysis. A pure KBr pellet was used as the reference baseline. The spectra were recorded in the range of 4000–400 cm⁻¹, and the absorption bands obtained were used to identify the characteristic functional groups associated with dietary fibre.²⁶

2.7.3 X-ray diffraction pattern (XRD). The X-ray diffraction pattern was recorded using an X-ray diffractometer (Bruker AXS D8, Bruker Inc., Germany). The diffraction angles were scanned over a 2θ range of 5° to 80°, and the instrument was operated at a peak voltage of 35 kV and current of 32 mA.²⁶

2.8 Statistical analysis

Statistical analyses were performed using Analysis of Variance (ANOVA) with the Statistical Package for Social Sciences (SPSS), version 21 (IBM SPSS Inc., Chicago, IL). The experiment was conducted in triplicate using a completely randomised design, and the results are expressed as the mean ± standard deviation of the replicates. Duncan's multiple range test was used to compare means at a significance level of $p < 0.05$.



Table 1 Proximate analysis of dietary fibre extracted from banana pseudostem scutcher from different methods^a

Parameter	CHE	HWE	MAE	UAE	UAE + MAE
Moisture (%)	5.58 ± 0.54 ^b	9.8 ± 0.28 ^a	4.71 ± 0.24 ^c	3.67 ± 0.28 ^e	3.35 ± 0.06 ^f
<i>a_w</i>	0.47 ± 0.01 ^b	0.52 ± 0.01 ^a	0.43 ± 0.05 ^c	0.44 ± 0.04 ^d	0.46 ± 0.05 ^c
Extraction recovery (%)	97.95 ± 0.15 ^a	80.54 ± 0.81 ^e	93.41 ± 2.61 ^c	92.78 ± 0.54 ^d	96.25 ± 2.15 ^b
True dietary fibre yield (%)	74.27 ± 1.17 ^b	50.54 ± 2.38 ^e	73.79 ± 2.83 ^{ab}	76.24 ± 1.04 ^b	81.67 ± 0.82 ^a
Carbohydrate (%)	76.25 ± 3.01 ^d	73.82 ± 2.73 ^e	81.49 ± 3.19 ^c	84.06 ± 4.42 ^a	85.02 ± 1.95 ^b
Ash (%)	14.23 ± 0.37 ^a	15.56 ± 0.46 ^b	10.23 ± 0.9 ^c	11.56 ± 0.28 ^d	11.02 ± 0.66 ^c
Fat (%)	0.76 ± 0.01 ^a	0.63 ± 0.01 ^b	0.49 ± 0.09 ^c	0.65 ± 0.01 ^c	0.63 ± 0.01 ^b
Protein (%)	0.18 ± 0.08 ^b	0.19 ± 0.01 ^a	0.08 ± 0.3 ^c	0.07 ± 0.04 ^d	0.06 ± 0.04 ^c
Total phenolics (mg GAE/100 g)	52.67 ± 1.66 ^c	46.19 ± 1.54 ^f	65.48 ± 1.6 ^c	72.5 ± 3.26 ^b	95.07 ± 1.68 ^a
Total flavonoids (mg QE/100 g)	29.92 ± 1.07 ^d	21.45 ± 1.15 ^e	31.43 ± 1.07 ^c	43.92 ± 1.3 ^b	65.67 ± 1.36 ^a
TDF (%)	75.85 ± 1.01 ^d	62.75 ± 1.73 ^e	78.99 ± 1.19 ^c	82.15 ± 1.95 ^b	84.85 ± 1.42 ^a
IDF (%)	56.14 ± 0.76 ^d	45.81 ± 1.30 ^e	58.49 ± 0.89 ^c	61.11 ± 1.46 ^b	60.64 ± 1.07 ^a
SDF (%)	19.71 ± 0.25 ^d	16.94 ± 0.43 ^e	20.50 ± 0.30 ^c	21.04 ± 0.49 ^b	24.21 ± 0.36 ^a

^a Data presented are mean values ± standard deviation ($n = 3$). Different superscripts in the same row are significantly different ($p < 0.05$) according to Duncan's multiple range test. CHE (chemical), HWE (hot water extraction), MAE (microwave assisted), UAE (ultrasound assisted), UAE + MAE (ultrasound + microwave), TDF: total dietary fibre, IDF: insoluble dietary fibre, and SDF: soluble dietary fibre.

3 Results and discussion

3.1 Proximate composition

The extraction recovery and true dietary fibre yield varied significantly among the different techniques employed (Table 1). Extraction recovery ranged from 80.54 ± 0.81% to 97.95 ± 0.15%, while true dietary fibre yield varied between 50.54 ± 2.38% and 81.67 ± 0.82%. Among the green methods, HWE resulted in the lowest yield (80.54 ± 0.81%), which is attributable to limited cell wall disruption under mild aqueous conditions. Similar limitations of aqueous extraction in lignocellulosic matrices have been reported due to restricted solvent accessibility and intact fibre structure.²⁷ MAE and UAE considerably enhanced the extraction yield to 93.41 ± 0.61% and 92.78 ± 0.54%, respectively (Table 1). These improvements can be attributed to rapid heating by microwaves, which causes intracellular pressure build-up and cell rupture,³⁶ resulting in enhanced mass transfer and release of bound polysaccharides,³⁷ and to ultrasonic cavitation, which facilitates solvent penetration and matrix disintegration.

The combination of UAE and MAE produced an even higher yield of 95.62 ± 0.43%, suggesting a synergistic effect between microwave-induced thermal energy and mechanical shear forces from ultrasonic waves that accelerates mass transfer and promotes efficient fibre release.³⁷ Such synergistic effects have been widely reported in hybrid extraction systems, where combined physical forces improve extraction kinetics and structural disruption.³⁸ Although CHE extraction demonstrated a comparatively higher yield, its use of alkali may lead to partial hydrolysis of polysaccharides and degradation of thermolabile compounds, making it less desirable for clean-label or food-grade applications. Alkaline treatments are known to solubilise hemicellulose and disrupt lignin linkages, but may also alter the fibre structure and reduce bioactive retention. Similar trends were observed in previous studies, where Wang *et al.*, 2021⁷ reported that alkaline-assisted extraction (ALE) resulted in the highest TDF and SDF yields (92.88% and 32.85%,

respectively) due to extensive cell wall disruption and partial solubilisation of hemicellulose, converting IDF into SDF.

3.2 Dietary fibre

In the present study, the dual method, UAE + MAE treatment, resulted in the highest recovery of total dietary fibre (TDF), showing nearly a 35% increase compared with the HWE process, and about 10–12% higher than conventional chemical extraction, demonstrating the clear advantage of integrating ultrasound and microwave energy. Similar enhancements in TDF recovery using combined physical treatments have been reported for plant residues due to improved disruption of lignocellulosic matrices.³⁸ This improvement is linked to the combined effects of cavitation and microwave-induced thermal pressure, which effectively rupture cell walls and release bound polysaccharides. These mechanisms facilitate the breakdown of hydrogen bonds and increase solvent accessibility to cellulose and hemicellulose fractions.³⁷ UAE alone yielded a markedly higher proportion of insoluble dietary fibre (IDF), with nearly a 30% increase over HWE treatment, indicating enhanced liberation of cellulose, hemicellulose, and lignin components. Increased IDF recovery following ultrasonic treatment has been associated with mechanical disruption of fibre bundles and exposure of structural polysaccharides.³⁹ UAE + MAE also improved soluble dietary fibre (SDF) by approximately 40% over hot water extraction, reflecting its efficiency in solubilising pectins and β-glucans without excessive degradation. Microwave treatment is known to promote partial depolymerisation of polysaccharides, enhancing SDF formation.²⁰ The balance between SDF and IDF was more desirable in UAE + MAE, indicating improved functional attributes such as hydration and binding capacity. A balanced SDF/IDF ratio is critical for improving the physiological and techno-functional properties of dietary fibre.⁴⁰ In contrast, HWE resulted in the lowest fibre content and poorer functional quality due to prolonged heating, leading to partial solubilization and thermal degradation of structural polysaccharides. These findings emphasise that



Table 2 Colourimetric analysis and flow properties of dietary fibre extracted from banana pseudostem scutcher from various methods^a

	CHE	HWE	MAE	UAE	UAE + MAE
<i>L</i> *	49.37 ± 0.01 ^c	44.09 ± 0.02 ^e	51.07 ± 0.01 ^b	53.14 ± 0.02 ^a	42.42 ± 0.01 ^f
<i>a</i> *	7.34 ± 0.01 ^a	3.83 ± 0.01 ^e	5.16 ± 0.03 ^d	5.23 ± 0.01 ^c	5.87 ± 0.01 ^b
<i>b</i> *	20.79 ± 0.04 ^a	10.46 ± 0.01 ^e	16.52 ± 0.02 ^d	17.51 ± 0.01 ^c	17.58 ± 0.02 ^b
<i>h</i>	70.53 ± 0.03 ^d	69.91 ± 0.05 ^e	72.64 ± 0.01 ^b	73.34 ± 0.04 ^a	71.53 ± 0.02 ^c
<i>C</i> *	22.05 ± 0.01 ^a	11.13 ± 0.01 ^e	17.31 ± 0.02 ^d	18.27 ± 0.01 ^c	18.54 ± 0.01 ^b
Bulk density	0.24 ± 0.01 ^b	0.31 ± 0.02 ^a	0.19 ± 0.02 ^d	0.21 ± 0.01 ^c	0.21 ± 0.03 ^c
Tapped density	0.31 ± 0.04 ^b	0.38 ± 0.04 ^a	0.22 ± 0.04 ^d	0.24 ± 0.06 ^c	0.24 ± 0.07 ^c
Carr index (%)	22.6 ± 1.02 ^a	18.4 ± 1.0 ^b	13.6 ± 1.4 ^c	12.5 ± 1.6 ^d	12.5 ± 2.1 ^d
Hausner ratio	1.29 ± 0.05 ^a	1.23 ± 0.07 ^b	1.16 ± 0.05 ^c	1.14 ± 0.03 ^d	1.14 ± 0.02 ^d

^a Data presented are mean values ± standard deviation ($n = 3$). Different superscripts in the same row are significantly different ($p < 0.05$) according to Duncan's multiple range test. CHE (chemical), HWE (hot water extraction), MAE (microwave assisted), UAE (ultrasound assisted), and UAE + MAE (ultrasound + microwave).

hybrid physical-assisted extraction notably enhanced both the quantity and functional integrity of dietary fibre compared to conventional processes.

3.3 Colour

The colour attributes of dietary fibre (DF) differed significantly ($p < 0.05$) among the various extraction methods (Table 2). The highest *L** value, indicating maximum lightness, was observed in UAE-treated DF (53.14 ± 0.02), reflecting a brighter and less pigmented appearance. In contrast, the combined UAE + MAE treatment exhibited the lowest *L** value (42.42 ± 0.01), suggesting increased browning or pigment retention. This reduction in lightness may be attributed to intensified extraction conditions promoting pigment release. Additionally, non-enzymatic browning reactions and thermal degradation of natural pigments under microwave conditions may contribute to darker coloration. The *a** value, representing redness, was significantly higher in the chemically extracted (CHE) sample (7.34 ± 0.01), likely due to pigment oxidation or retention of colour compounds during alkali treatment. Conversely, hot-water extraction (HWE) resulted in the lowest *a** and *b** values, indicating a lighter and less yellowish fiber, possibly due to pigment degradation or leaching during thermal processing. The *b** value and chroma (*C**), which denote yellowness and color intensity, were also highest in chemically treated samples, confirming more saturated coloration. The hue angle (*h*°) ranged between 69.91° and 73.34° , indicating a predominantly yellow tone across all samples, with UAE-treated DF maintaining the most stable hue, likely due to minimal thermal degradation of natural pigments by reducing thermal exposure.

3.4 Flow characteristics

The flow characteristics of the dietary fibre reflect the compressibility and cohesiveness of the powder, which directly influence its handling, mixing, and packaging behavior. The bulk density values ranged from 0.19 to 0.31 g cm^{-3} , with the HWE sample exhibiting the highest (0.31 g cm^{-3}) and MAE the lowest (0.19 g cm^{-3}). Higher bulk density indicates better packing ability and reduced porosity. This may be associated with particle size reduction and structural compaction during

thermal treatment. The tapped density followed a similar trend, with HWE showing the highest value (0.38 g cm^{-3}). The Carr Index, an indicator of powder flowability, varied between 12.5% and 22.6%. Among the treatments, UAE and UAE + MAE recorded the lowest CI (12.5%), signifying excellent flowability, whereas CHE showed the highest (22.6%), indicating poor flow due to particle agglomeration or irregular shape. Improved flow properties following physical treatments can be attributed to reduced particle cohesion and more uniform particle size distribution.⁴¹ Similarly, the Hausner ratio values ranged from 1.14 to 1.29. Values close to 1.0 denote free flowing powders, while those above 1.25 imply cohesive nature.²⁷ The UAE (1.14) and UAE + MAE (1.14) samples demonstrated the best flow properties, followed by MAE (1.16) and HWE (1.23), whereas CHE (1.29) exhibited the least favorable flow behaviour due to

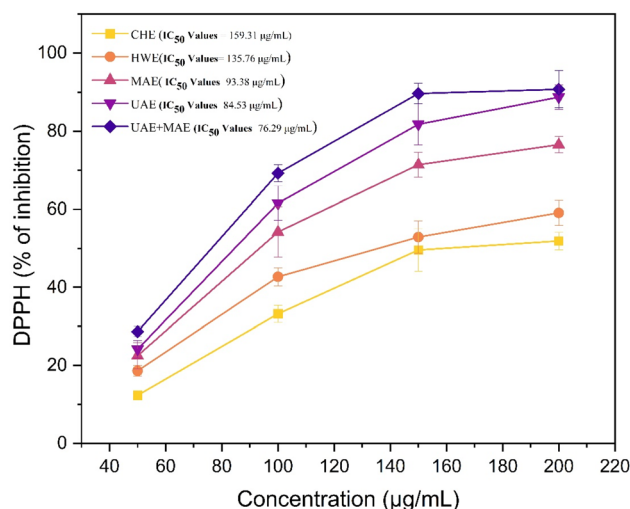


Fig. 1 Antioxidant potential of dietary fibre from banana pseudostem scutcher processed via different treatments. Data presented are mean values ± standard deviation ($n = 3$). Different superscripts in the same row are significantly different ($p < 0.05$) according to Duncan's multiple range test. CHE (chemical), HWE (hot water extraction), MAE (microwave assisted), UAE (ultrasound assisted), and UAE + MAE (ultrasound + microwave).



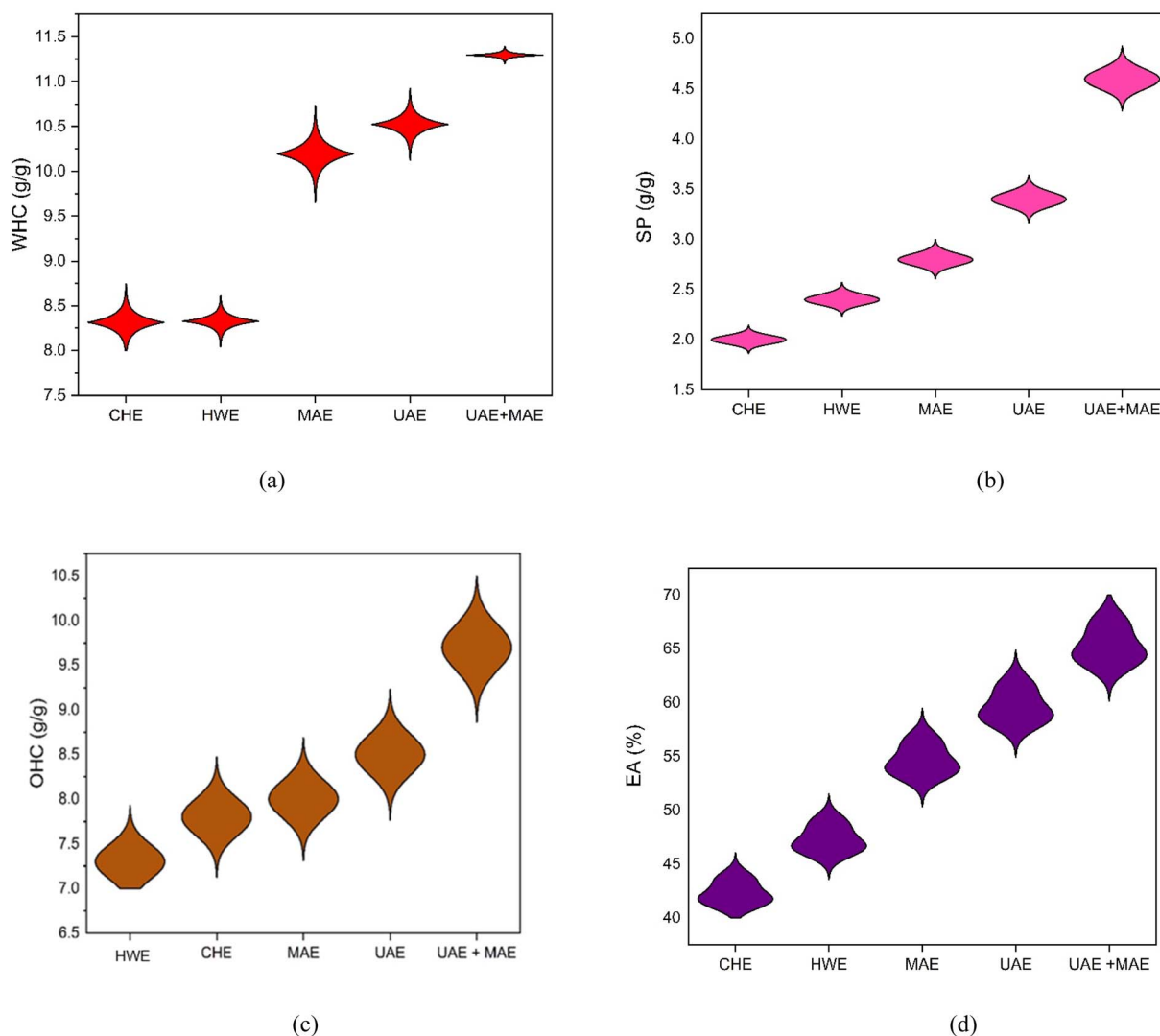


Fig. 2 Techno-functional properties of dietary fibre extracted from banana pseudostem scutcher extracted via different treatments: (a) water holding capacity, (b) swelling capacity, (c) oil holding capacity, and (d) emulsion activity. Data presented are mean values \pm standard deviation ($n = 3$). Different superscripts in the same row are significantly different ($p < 0.05$) according to Duncan's multiple range test. CHE (chemical), HWE (hot water extraction), MAE (microwave assisted), UAE (ultrasound assisted), and UAE + MAE (ultrasound + microwave).

irregular particle morphology and higher surface roughness caused by chemical degradation of structural components.

3.5 Secondary metabolites

The extraction techniques markedly influenced the phenolic and flavonoid constituents of dietary fibre. Total phenolic content (TPC) ranged from 46.19 ± 1.54 to 95.07 ± 1.68 mg GAE/100 g, whereas total flavonoid content (TFC) varied between 21.45 ± 1.15 and 65.67 ± 1.36 mg QE/100 g. The highest values for both parameters were obtained in UAE + MAE treatment. Similar findings have been reported where combined extraction techniques enhanced the release of bound phenolics through cell wall disruption³⁸ and rapid dielectric heating enhanced the release of matrix-bound polyphenols.¹⁸ Ultrasound generates cavitation, which weakens lignocellulosic fibres and improves solvent penetration, while microwave-assisted heating

promotes cell wall rupture and diffusion of solutes.^{37,42} Conversely, phenolic and flavonoid content was lower in chemically and water-based extractions, likely due to oxidative and hydrolytic degradation of polyphenols under prolonged heating or alkaline pH.⁴³

The antioxidant activity of the fibre extracts, expressed as DPPH radical scavenging capacity (Fig. 1), demonstrated a clear concentration-dependent increase from 50 to $200 \mu\text{g mL}^{-1}$. At $50 \mu\text{g mL}^{-1}$, inhibition ranged from 18.2% to 58.7%, while at $200 \mu\text{g mL}^{-1}$, inhibition increased to 55.9% to 79.5%, indicating a strong ability of the extracts to donate hydrogen atoms or electrons to neutralise free radicals. Numerous studies support this positive association between TPC, TFC and DPPH activity.^{44,45} US-MWE extracted DF possessed loose and porous structures and reduced molecular weight, which might have facilitated the donation of electrons, forming stable free radicals and terminating free radical reactions.³²



3.6 Techno-functional characterisation

3.6.1 Hydration properties and oil holding capacity. The hydration and lipid-binding properties of dietary fibre varied markedly with the extraction technique employed. Dual treatment, a combination of UAE + MAE, significantly enhanced water-holding capacity (WHC) (Fig. 2a), oil-holding capacity (OHC) (Fig. 2c), and swelling power (SP) (Fig. 2b) compared to conventional and single step methods. Fibres extracted through UAE + MAE demonstrated the highest functional properties, approximately 20–30% higher than chemically extracted samples and nearly double those of hot water extraction. This improvement was not solely due to cavitation and thermal pressure but rather to the complementary mechanisms of both technologies. Together, they generated a more open, sponge-like matrix with greater internal voids and accessible binding sites. Similar structural modifications leading to enhanced hydration properties have been reported for ultrasound- and microwave-treated plant fibres due to disruption of hydrogen bonding and increased surface area.^{37,38} This structural transformation probably facilitated the entrapment of water within capillaries and enhanced oil absorption by exposing nonpolar sites on cellulose, hemicellulose, and lignin.⁴⁶

UAE alone also significantly improved WHC, OHC, and SP compared to MAE and chemical extraction, indicating that mechanical effects such as microjets and shear forces are more effective in modifying fibre topology. Ultrasonic cavitation has been shown to increase pore volume and surface roughness, thereby improving water and oil retention capacity.³⁹ In contrast, MAE-treated fibres showed moderate improvements, suggesting that thermal softening alone is less effective without mechanical disruption. The lowest values observed in HWE may be attributed to prolonged heating, which can lead to structural compaction and partial depolymerisation, thereby reducing capillary spaces. Thermal treatments have been reported to collapse porous structures and reduce the functional properties of dietary fibres.⁴⁰

The significantly higher swelling capacity of UAE + MAE-treated fibres indicates enhanced internal hydration zones and improved diffusion pathways. Such structural features are associated with improved physiological functionality, including delayed gastric emptying, reduced glucose diffusion, and increased satiety.⁴⁰ Prolonged exposure to high temperatures may have compacted fibre structures or triggered partial depolymerisation, resulting in reduced capillary spaces and fewer active sites capable of retaining water and lipids.⁴⁷ Notably, the swelling capacity of UAE + MAE-treated fibres was nearly twice that of chemically extracted samples. This behaviour suggests increased internal hydration zones and improved diffusion channels that facilitate water penetration and swelling, including delayed gastric emptying, reduced glucose diffusion, and increased satiety.²²

3.6.2 Emulsification activity. The emulsifying activity (EA) results (Fig. 2d) showed the lowest values for CHE (42%) and the highest for UAE + MAE (65%). Treatments such as HWE (47%), MAE (55%), and UAE (59%) displayed intermediate improvements. The enhancement in EA following modification is likely

related to the exposure of hydrophilic and hydrophobic groups within the fibre matrix, which facilitates interfacial adsorption and stabilisation of oil-water emulsions. Ultrasound and microwave treatments are known to partially depolymerise polysaccharides and increase surface-active groups, thereby improving emulsification properties.³² Dietary fibres with strong emulsifying capacity can be valuable in food applications, acting as natural stabilisers, while also conferring physiological benefits such as cholesterol reduction by binding bile salts and lipids.¹⁴ The significantly higher EA of UAE + MAE-treated fibre further supports the hypothesis that combined modification improves functional properties more effectively than individual treatments.

3.7 Bioactive adsorption analysis

3.7.1 Cholesterol adsorption capacity. Dietary fibre's capacity to adsorb cholesterol plays a significant role in lowering blood cholesterol levels, particularly LDL cholesterol, by binding to bile acids and preventing their reabsorption, thereby promoting cardiovascular health.³ The cholesterol adsorption capacity (CAC) of dietary fibres obtained through different extraction methods showed significant variation under both acidic (pH 2.0) and neutral (pH 7.0) conditions (Fig. 3c). The pH-dependent variation observed in this study aligns with the physiological environment, where fibres can bind cholesterol in both the stomach and small intestine, though efficiency tends to decrease under neutral conditions. Among the treatments, UAE + MAE fibre exhibited the highest CAC, being about 2.3-fold higher at pH 2.0 and 3.2-fold higher at pH 7.0 compared to HWE. UAE-treated fibre showed an increase of approximately 2.1-fold (pH 2.0) and 2.6-fold (pH 7.0), while MAE achieved around 1.7-fold (pH 2.0) and 2.2-fold (pH 7.0). In contrast, CHE treatment displayed only a modest improvement, with CAC values 1.4 times higher at pH 2.0 and 1.3 times higher at pH 7.0 than HWE. These results suggest that combined microwave and ultrasonic and ultrasonic-assisted extractions effectively modified fibre structures to enhance cholesterol-binding sites, likely by increasing porosity and exposing active functional groups. Increased porosity, surface area, and exposure of functional groups such as hydroxyl and carboxyl groups enhance cholesterol adsorption through physical entrapment and electrostatic interactions. These findings are consistent with earlier reports that soluble dietary fibre (SDF) generally exhibits higher CAC than insoluble dietary fibre (IDF) due to its greater swelling capacity and gel forming ability.²⁰ In kiwifruit derived fibres, AC-SDF showed the highest CAC at both pH 2.0 (29.42 mg g⁻¹) and pH 7.0 (22.68 mg g⁻¹), significantly higher than IDF fractions.⁷ The higher CAC of SDF is attributed to its looser structure, increased surface area, and presence of hydrophilic groups, which enable cholesterol binding through both physical entrapment and molecular interactions.

3.7.2 Nitrite ion adsorption capacity. The adsorption of nitrite ions by dietary fibre is important for detoxifying potentially harmful substances such as nitrosamines in the body, found in processed foods, and may help reduce the risk of nitrosamine formation, which is linked to cancer. The nitrite



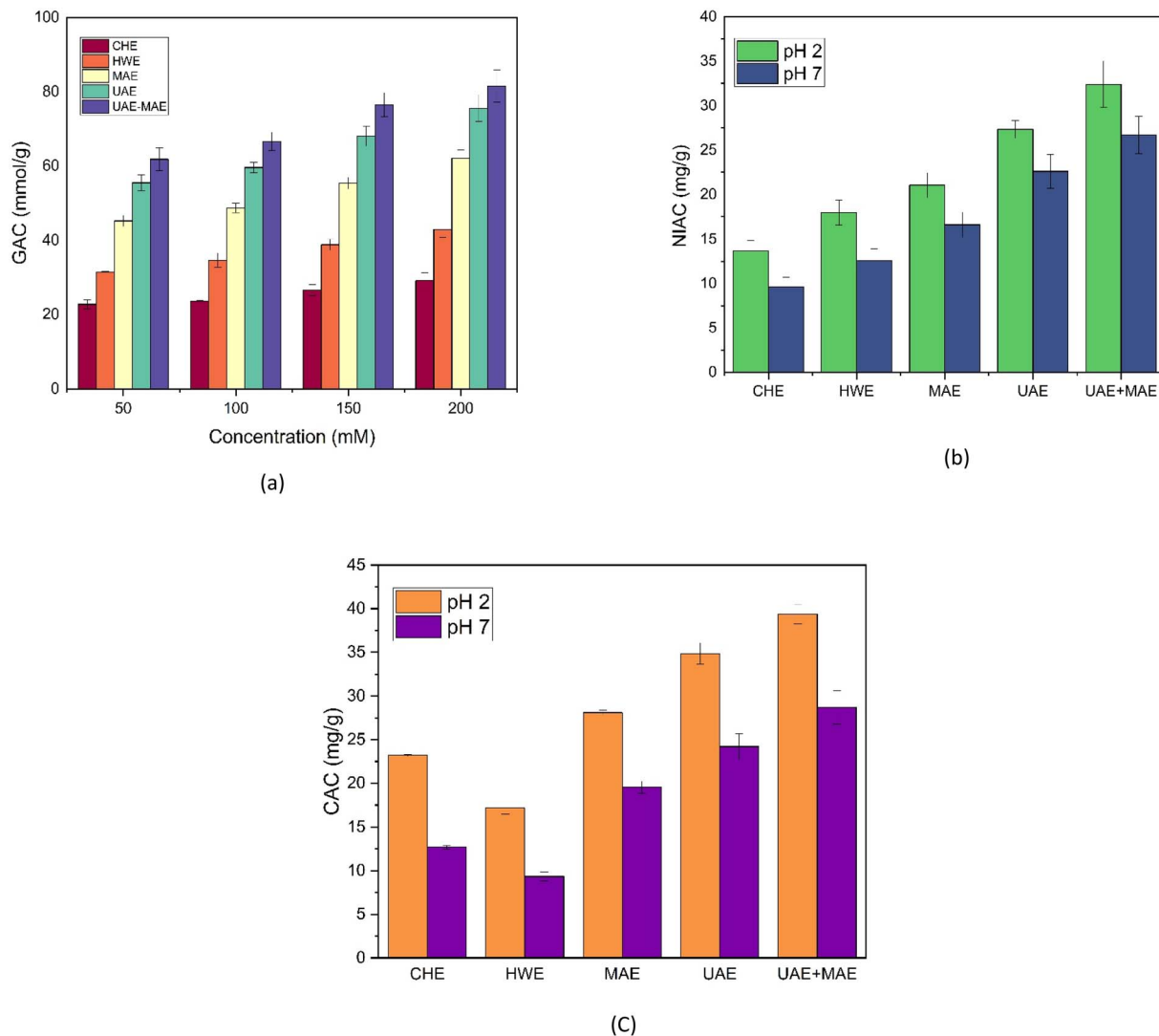


Fig. 3 Bioactive compound adsorption by banana pseudostem scutcher dietary fibre obtained using different extraction methods: (a) glucose adsorption capacity, (b) nitrite ion adsorption capacity, and (c) cholesterol adsorption capacity. Data presented are mean values \pm standard deviation ($n = 3$). Different superscripts in the same row are significantly different ($p < 0.05$) according to Duncan's multiple range test. CHE (chemical), HWE (hot water extraction), MAE (microwave assisted), UAE (ultrasound assisted), and UAE + MAE (ultrasound + microwave).

ion adsorption capacity (NIAC) of dietary fibre extracted from banana scutcher was examined under simulated gastric (pH 2) and intestinal (pH 7) conditions (Fig. 3b). Across all treatments, adsorption was significantly higher at pH 2 than at pH 7, indicating stronger binding under acidic conditions. This is consistent with earlier reports that acidic environments enhance the protonation of functional groups, thereby promoting ionic interactions between fibre matrices and nitrite ions. Modified dietary fibres with higher porosity and swelling capacity exhibit improved glucose adsorption and diffusion retardation. Among the extraction methods, CHE fibre showed the lowest NIAC values (13.5 mg g^{-1} at pH 2 and 9.5 mg g^{-1} at pH 7), whereas the UAE + MAE treatment achieved the highest adsorption (32.8 mg g^{-1} at pH 2 and 26.9 mg g^{-1} at pH 7).³⁸ HWE and MAE extractions produced moderate capacities, ranging from $17.9\text{--}21.2 \text{ mg g}^{-1}$ at pH 2 and $12.6\text{--}16.8 \text{ mg g}^{-1}$ at

pH 7. UAE fibre displayed notably higher NIAC (27.5 mg g^{-1} at pH 2; 22.8 mg g^{-1} at pH 7), second only to UAE + MAE. The enhanced nitrite-binding efficiency in UAE and UAE + MAE-treated fibres can be attributed to extensive structural modifications, such as increased porosity, reduced crystallinity, and exposure of hydroxyl and carboxyl functional groups, as confirmed by SEM and FTIR analyses in this study. These alterations increase the availability of active adsorption sites for nitrite ions.

3.7.3 Glucose adsorption capacity. The ability of DF to adsorb glucose is essential for regulating blood sugar levels, as it can slow down carbohydrate digestion and absorption, thereby preventing rapid spikes in blood glucose.⁴ This property makes DF a key component in managing conditions like diabetes. In this study, a consistent concentration-dependent increase in GAC was observed in all treatments, indicating



that higher glucose levels enhanced fibre glucose interactions (Fig. 3a). However, significant differences were noted among the extraction methods. At 50 mM glucose, the chemically extracted (CHE) fibre exhibited the lowest adsorption (22.4 mmol g^{-1}), while the combined ultrasound-microwave (UAE + MAE) treatment showed the highest (61.7 mmol g^{-1}). Hot water extracted (HWE) and microwave-assisted (MAE) extractions produced intermediate values (31.6 and 45.2 mmol g^{-1} , respectively), whereas ultrasound-assisted (UAE) extraction yielded 55.4 mmol g^{-1} . This trend persisted across all treatments, with UAE + MAE consistently outperforming other treatments. At

200 mM , UAE + MAE reached a maximum GAC of 81.2 mmol g^{-1} , nearly 2.8-fold higher than CHE (28.9 mmol g^{-1}) and significantly greater than HWE (42.8 mmol g^{-1}), MAE (61.5 mmol g^{-1}), and UAE (74.3 mmol g^{-1}).

3.8 Morpho-structural analysis

3.8.1 Morphology examination. As shown in Fig. 4, the morphological and functional characteristics of dietary fibre derived from banana fibre scutcher were strongly influenced by the pre-processing treatments. Chemical treatment with NaOH led to rough, cracked surfaces due to alkaline hydrolysis of

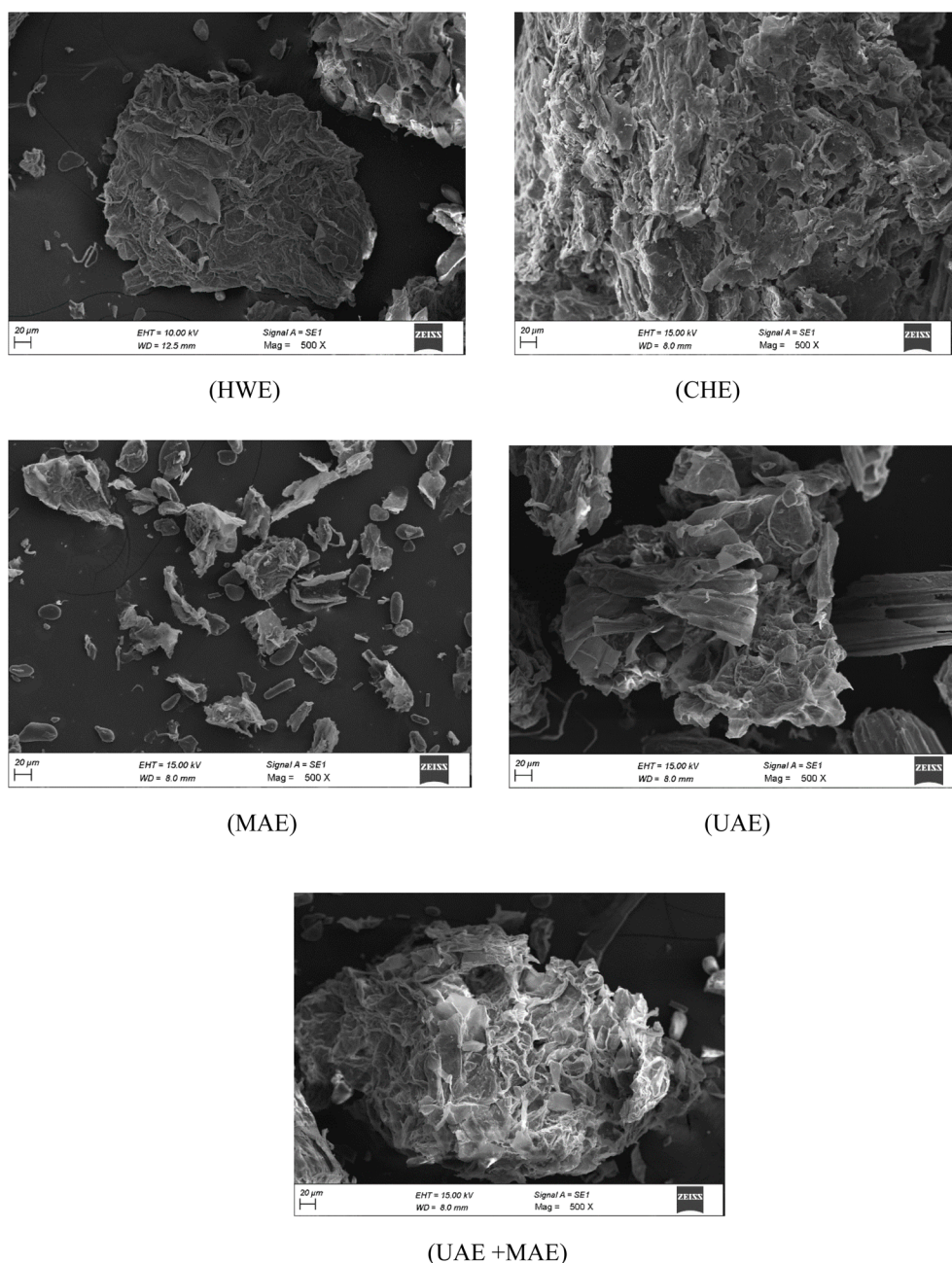


Fig. 4 Morphological characterisation of dietary fibre from banana pseudostem scutcher extracted *via* various treatments (500X magnification): CHE (chemical), HWE (hot water extraction), MAE (microwave assisted), UAE (ultrasound assisted), and UAE + MAE (ultrasound + microwave).



hemicellulose and partial solubilisation of lignin, which disrupted the cellulose, hemicellulose, lignin matrix and exposed fibrillar structures, thereby enhancing water- and oil-binding capacities. Hot water extraction, in contrast, produced smoother, denser, and more compact fibres; the high-temperature water partially gelatinised amorphous components while leaving the cellulose framework largely intact, limiting porosity and yielding only moderate improvements in swelling.²⁵ Microwave-assisted extraction generated highly porous and irregular surfaces, as rapid dipole rotation and internal heating caused cell wall rupture and collapse of compact structures, increasing surface area. Ultrasound-assisted extraction produced sponge-like porous structures through cavitation-induced erosion, where shear forces and microjets disrupted the fibre network. The combined UAE + MAE treatment exhibited the most pronounced disintegration, resulting in highly irregular fragments, extensive porosity, and exposed fibrillar networks due to the synergistic effects of internal microwave-induced rupture and external ultrasound-induced shear. This treatment corresponded to the greatest enhancements in water-holding capacity, oil-binding capacity, swelling ability, and bioactive extractability.³³

3.8.2 Functional group identification using FTIR. In the study, infrared spectroscopy analysis was used to detect the organic functional group. All samples exhibited a broad absorption band in the region of 3270–3300 cm^{-1} , attributed to the –OH stretching vibration of hydrogen-bonded hydroxyl groups in polysaccharides (Fig. 5). This band was sharp and intense in the HWE sample, indicating well preserved hydrogen bonding within the cellulose structure. Conversely, the UAE + MAE sample displayed a broadened and less intense OH peak, reflecting disruption of hydrogen bonds and increased exposure of hydroxyl groups, which is beneficial for hydration and swelling properties. These changes align with observations by Ma & Mu *et al.*¹² and Chen *et al.*,⁵⁰ who noted that the broad OH band is sensitive to hydrogen bonding alterations due to

physical or chemical treatments. The absorption bands in the 2920–2850 cm^{-1} region correspond to the C–H stretching vibrations of methylene (–CH₂) groups. Minimal variation was observed across samples; however, a slight intensity decrease in the UAE + MAE sample suggests surface modifications and partial cleavage of aliphatic chains, consistent with previous reports by Ma & Mu *et al.*¹² A strong absorption peak at 1730 cm^{-1} , attributed to the C=O stretching vibration of ester or carboxyl groups, was most prominent in the CHE treated samples. This indicates the exposure of esterified carboxyl groups due to the degradation of hemicellulose and pectin during chemical hydrolysis. Structural breakdown of polysaccharides improves functional properties such as swelling and adsorption.³⁹

Reduced intensity of this band in the UAE and MAE samples suggests partial removal of hemicellulose and lignin, corroborated by a concurrent decrease in crystallinity observed in XRD results. Similar findings were reported by Li *et al.*,⁴⁸ who linked such spectral changes to the breakdown of lignocellulosic structures. In the 1200–1400 cm^{-1} region, assigned to CH bending and variable angle vibrations, characteristic peaks of polysaccharides were present in all samples, reflecting typical saccharide structures in both insoluble (IDF) and soluble dietary fibres (SDF). The 1050–1160 cm^{-1} region, characteristic of C–O–C and C–O–H stretching vibrations in carbohydrates, displayed sharp and intense peaks in the HWE sample, indicating a more ordered and intact cellulose structure. In contrast, these bands were broader and of lower intensity in the UAE and UAE + MAE samples, signifying structural disintegration and a shift toward a more amorphous fibre matrix. These modifications expose more active binding sites, which enhance the fibre's water and oil-holding capacities.⁴⁹ Notably, the absorption peak around 890 cm^{-1} , indicative of β -glycosidic linkages in cellulose, was reduced in intensity in the UAE and UAE + MAE samples. This implies partial depolymerisation of the cellulose backbone due to ultrasonic cavitation and microwave-induced heating. According to Chen *et al.*,⁵⁰ the weakening of this band reflects a disruption in the β -pyranose structure, a hallmark of fibre modification leading to improved hydration and swelling properties. Furthermore, Li *et al.*⁴⁸ noted that the region between 1000 and 700 cm^{-1} contains absorption bands corresponding to α - and β -anomers in monosaccharides. The changes observed in these bands in the treated fibres, especially in the UAE + MAE sample, confirm molecular restructuring. The presence of xylan was confirmed by the C–O stretching vibration peak around 1000 cm^{-1} , indicating that hemicellulose remained part of the dietary fibre matrix.⁵⁰

3.8.3 XRD characterization. X-ray diffraction (XRD) analysis revealed characteristic peaks at $2\theta \approx 15\text{--}16^\circ$ and 22° , with minor peaks around $34\text{--}35^\circ$, confirming the presence of cellulose I crystalline structure in all samples (Fig. 6). These peaks correspond to the ordered crystalline regions of native cellulose within the fibre matrix (Sun *et al.*⁴⁹). The HWE sample exhibited sharp and well-defined peaks, indicating high crystallinity and tightly packed cellulose chains. This ordered arrangement limits the accessibility of hydroxyl groups, which explains its

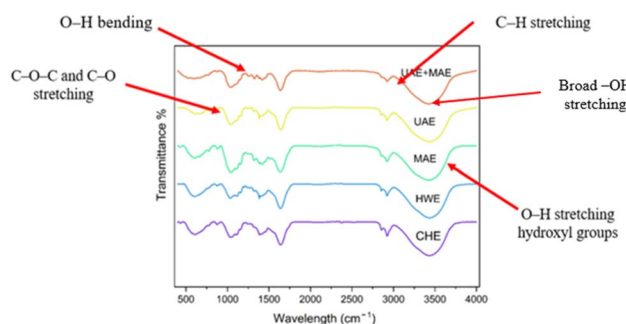


Fig. 5 FTIR spectra of dietary fibre obtained via different extraction treatments. A progressive decrease in –OH stretching band intensity and peak broadening from HWE to UAE + MAE indicates disruption of hydrogen bonding and increased exposure of reactive hydroxyl groups. Reduction in β -glycosidic and C–O–C band intensities further confirms partial depolymerisation and structural disintegration of the lignocellulosic matrix: CHE (chemical), HWE (hot water extraction), MAE (microwave assisted), UAE (ultrasound assisted) and UAE + MAE (ultrasound + microwave).



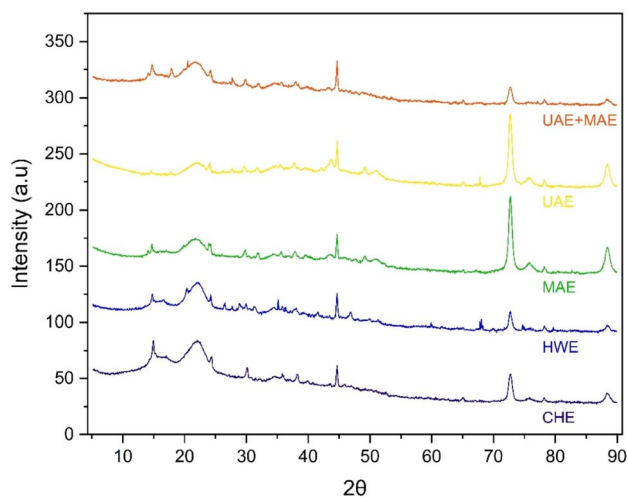


Fig. 6 X-ray diffraction (XRD) patterns of dietary fibre obtained from banana pseudostem scutcher via different extraction treatments: CHE (chemical), HWE (hot water extraction), MAE (microwave assisted), UAE (ultrasound assisted), and UAE + MAE (ultrasound + microwave).

compact morphology (SEM) and lower water holding capacity (WHC) and swelling behaviour.

In contrast, the CHE sample showed reduced peak intensity, suggesting partial disruption of crystalline domains and formation of amorphous regions. This enhances solvent accessibility and correlates with improved functional properties, although the persistence of distinct peaks indicates retained structural rigidity. MAE-treated samples displayed broader peaks, particularly at $2\theta \approx 22^\circ$, indicating reduced crystallinity due to disruption of intra- and intermolecular hydrogen bonding by dielectric heating. Similar reductions in crystallinity have been reported by Gan *et al.*,³³ reflecting increased molecular disorder and improved extractability of fibre components. UAE treatment resulted in further peak broadening and intensity reduction, indicating enhanced amorphisation due to cavitation-induced shear forces. This is consistent with Rawat *et al.*,²⁹ who reported that ultrasonic treatment reduces the degree of polymerisation and enhances solubility and binding capacity of dietary fibres. Increased amorphous regions improve water diffusion, swelling, and adsorption capacity. The UAE + MAE treatment exhibited the most pronounced structural transformation, with the lowest crystallinity among all samples. Extensive peak broadening suggests conversion of crystalline cellulose into amorphous regions, thereby increasing surface area and availability of active sites. Such reductions in crystallinity are strongly associated with enhanced hydration, oil-binding, and adsorption properties of dietary fibres. The XRD results are further supported by FTIR analysis, where increased $-OH$ stretching intensity in UAE and UAE + MAE samples indicates greater exposure of hydroxyl groups due to crystalline breakdown. This structural modification enhances fibre-water interactions and contributes to improved techno-functional and bioactive adsorption properties.

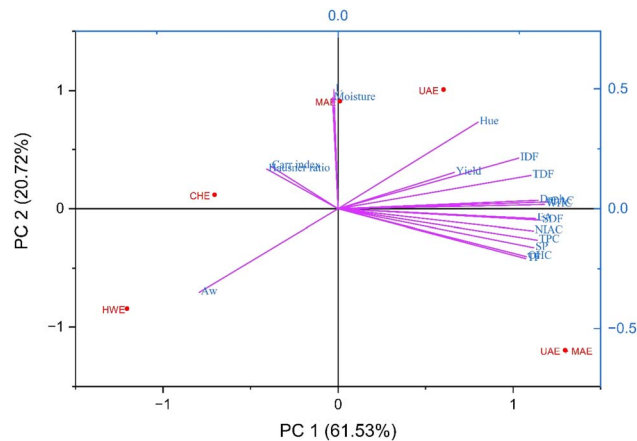


Fig. 7 Principal component analysis of dietary fibre from banana pseudostem scutcher obtained via different extraction methods: CHE (chemical), HWE (hot water extraction), MAE (microwave assisted), UAE (ultrasound assisted), and UAE + MAE (ultrasound + microwave).

4 Relationship among the observations

4.1 Principal component analysis

Principal component analysis (PCA) was employed to interpret the interrelationships between the compositional and functional attributes of dietary fibre extracted using different techniques. The first two principal components, PC1 (61.53%) and PC2 (20.72%), cumulatively explained 82.25% of the total variance, effectively differentiating the extraction treatments based on their physicochemical and techno-functional behaviour (Fig. 7). The biplot revealed a clear separation among treatments, with UAE + MAE positioned far along the positive axis of PC1, indicating a strong association with total dietary fibre (TDF), soluble (SDF) and insoluble dietary fibre (IDF) fractions, total phenolic content (TPC), and antioxidant activities (DPPH, FRAP, and ABTS).⁴⁴ This suggests that the synergistic effects of ultrasound and microwave irradiation enhanced mass transfer and cell wall disruption, leading to higher fibre yield and bioactive compound retention. Conversely, HWE appeared on the negative side of PC1 and PC2, correlating with higher water activity (*aw*) but reduced yield and phenolic content, likely due to thermal degradation and leaching effects. CHE and MAE were positioned near the origin, indicating intermediate efficiency and balanced bulk properties, such as Carr index and Hausner ratio, reflecting moderate flow and compaction characteristics. UAE aligned positively with fibre yield and colour stability (*hue*), signifying efficient extraction while maintaining structural integrity.

4.2 Heat map studies

A correlation heat map was constructed to visualise the interrelationships among the compositional, physicochemical, and functional parameters of dietary fibres extracted via different treatments (Fig. 8). The heat map revealed a strong positive correlation among total dietary fibre (TDF), insoluble dietary



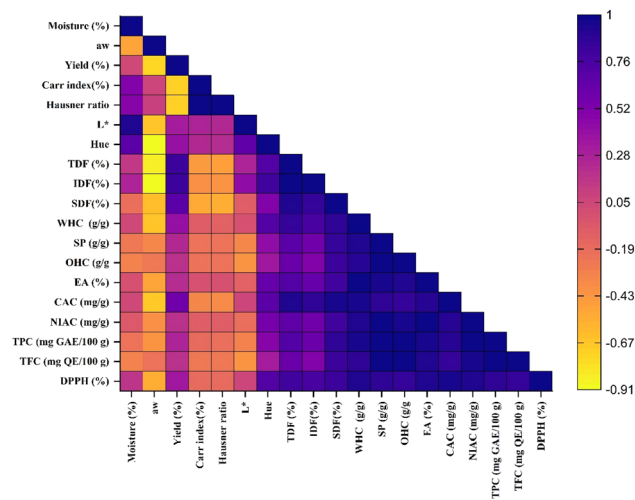


Fig. 8 Heat map representation of dietary fibre properties from banana pseudostem scutcher obtained via different extraction methods: CHE (chemical), HWE (hot water extraction), MAE (microwave assisted), UAE (ultrasound assisted), and UAE + MAE (ultrasound + microwave).

fibre (IDF), and soluble dietary fibre (SDF), indicating that the extraction efficiency of one fibre fraction positively influenced the others, reflecting the structural integrity and completeness of fibre recovery. Similarly, total phenolic content (TPC) exhibited a high degree of correlation with TDF and SDF, implying that phenolic compounds were tightly bound to the fibre matrix and co-extracted more efficiently under optimal extraction conditions, particularly under synergistic green treatment conditions.⁴⁵ Water-holding capacity (WHC) and oil-holding capacity (OHC) displayed strong positive associations with SDF and antioxidant activity (EA), suggesting that the presence of soluble polysaccharides and phenolic–fibre conjugates enhanced the hydration and lipid-binding potential of the extracted fibres. In contrast, negative correlations were observed between the Carr Index (CI), Hausner Ratio (HR), and hydration-related properties (WHC and OHC), signifying that increased functional capacity improved powder flowability by reducing particle cohesiveness.²⁷ The hue value was negatively associated with TPC and DPPH, implying that samples with darker colouration (lower hue) had higher phenolic content and antioxidant activity, likely due to pigment accumulation. Flow-related parameters such as the Carr index and Hausner ratio exhibited negative correlations with WHC and SP, suggesting that improved hydration and swelling abilities correspond to better flow and lower compressibility. The yield also showed a negative correlation with the Carr index and Hausner ratio, further confirming that samples with higher recovery rates demonstrated better flowability. Overall, the correlation analysis reinforced the findings of PCA, demonstrating that hybrid extraction methods such as UAE + MAE not only improved fibre yield and phenolic retention but also enhanced techno-functional properties such as water and oil binding capacities. These strong inter-parameter correlations underscore the compositional–functional synergy within the extracted dietary fibre, emphasising the role of green extraction strategies in

developing nutritionally superior and process-efficient functional ingredients.

5 Conclusion

The present study demonstrated that banana pseudostem scutcher is a viable source of dietary fibre with properties significantly influenced by the extraction technique. Among the methods evaluated, the combined ultrasound and microwave treatment (UAE + MAE) yielded dietary fibres with the most pronounced structural modifications, characterised by reduced crystallinity and increased porosity. These changes were reflected in superior techno-functional properties, including higher water-holding capacity (6.42 g g^{-1}), oil-holding capacity (4.98 g g^{-1}), and swelling power (5.75 mL g^{-1}), compared to other treatments. Additionally, UAE + MAE-treated fibres exhibited enhanced adsorption capacities, with maximum cholesterol adsorption (3.2-fold increase), nitrite ion adsorption (32.8 mg g^{-1}), and glucose adsorption (81.2 mmol g^{-1}). Structural analyses (SEM, FTIR, and XRD) confirmed that these improvements were associated with partial disruption of the lignocellulosic matrix, leading to increased exposure of functional groups and development of amorphous regions.

Author contributions

PSK: conceptualization, investigation, methodological development, writing of the original draft, data management, obtaining funding and investigation; MB: writing of the original draft and use of software.

Conflicts of interest

The authors declare that they have no financial interests or personal relationships that could have affected the research reported in this paper.

Abbreviations

DF	Dietary fibre
CHE	Chemical extraction
HWE	Hot water extraction
UAE	Ultrasonic-assisted extraction
MAE	Microwave-assisted extraction
IDF	Insoluble dietary fibre
SDF	Soluble dietary fibre
TDF	Total dietary fibre
WHC	Water-holding capacity
OHC	Oil-holding capacity
SP	Swelling power
BD	Bulk density
TD	Tapped density
HR	Hausner ratio
CI	Carr's index
aw	Water activity
L^*	Lightness
a^*	+Redness/–greenness



b^*	+Yellowness/–blueness
C^*	Chroma
H^*	Hue angle
ΔE	Total colour difference
EA	Emulsifying activity
TPC	Total phenolic content
TFC	Total flavonoid content
DPPH	2,2-Diphenyl-1-picrylhydrazyl
GAE	Gallic acid equivalent
QE	Quercetin equivalent
GAC	Glucose adsorption capacity
NIAC	Nitrite adsorption capacity
CAC	Cholesterol adsorption capacity
SEM	Scanning electron microscopy
FTIR	Fourier transform infrared spectroscopy
XRD	X-ray diffraction
ANOVA	Analysis of variance

Data availability

The data can be obtained upon request to the authors.

Acknowledgements

The authors express their heartfelt gratitude to the Director, ICAR – National Research Centre for Banana, Tiruchirappalli, for providing the required facilities and support. The authors sincerely acknowledge the Indian Council of Agricultural Research (ICAR), New Delhi, for providing research funding. This research was funded by the National Agricultural Science Fund (NASF), ICAR, New Delhi, under the project F. No. NASF/FME-9038/2023-24. We also extend our thanks to the Functional Materials Laboratory (I-109), PSG Institute of Advanced Studies, for assistance with SEM analysis. Additionally, we acknowledge the National College Instrumentation Facility (NCIF), Tiruchirappalli, for granting access to the XRD instrumentation.

References

- 1 N. Reynolds, A. Akerman, S. Kumar, H. T. D. Pham, S. Coffey and J. Mann, *BMC Med*, 2022, **20**, 139, DOI: [10.1186/s12916-022-02328-x](https://doi.org/10.1186/s12916-022-02328-x).
- 2 E. C. Deehan, V. Mocanu and K. L. Madsen, *Nat. Rev. Gastroenterol. Hepatol.*, 2024, **21**, 301–318, DOI: [10.1038/s41575-023-00891-z](https://doi.org/10.1038/s41575-023-00891-z).
- 3 D. E. Threapleton, D. C. Greenwood, C. Evans, C. L. Cleghorn, C. Nykjaer, C. Woodhead and V. J. Burley, *Proc. Nutr. Soc.*, 2013, **72**, E253, DOI: [10.1136/bmj.f6879](https://doi.org/10.1136/bmj.f6879).
- 4 D. Dhingra, M. Michael, H. Rajput and R. T. Patil, *J. Food Sci. Technol.*, 2012, **49**, 255–266, DOI: [10.1007/s13197-011-0365-5](https://doi.org/10.1007/s13197-011-0365-5).
- 5 Grand View Research, *Dietary Fibers Market Size, Share & Trends Analysis Report, 2024–2030*, 2023.
- 6 Y. Zhu, J. Chu, Z. Lu, F. Lv, X. Bie, C. Zhang and H. Zhao, *J. Cereal Sci.*, 2018, **79**, 456–461.
- 7 K. Wang, M. Li, Y. Wang, Z. Liu and Y. Ni, *Food Hydrocoll.*, 2021, **110**, 106162, DOI: [10.1016/j.foodhyd.2020.106162](https://doi.org/10.1016/j.foodhyd.2020.106162).
- 8 C. Beres, S. P. Freitas, R. L. O. Godoy, D. C. R. de Oliveira, R. Deliza, M. Iacomini, C. Mellinger-Silva and L. M. C. Cabral, *J. Funct. Foods*, 2019, **56**, 276–285, DOI: [10.1016/j.jff.2019.03.014](https://doi.org/10.1016/j.jff.2019.03.014).
- 9 T. Happi Emaga, C. Robert, S. N. Ronkart, B. Wathélet and M. Paquot, *Bioresour. Technol.*, 2008, **99**, 4346–4354, DOI: [10.1016/j.biortech.2007.08.030](https://doi.org/10.1016/j.biortech.2007.08.030).
- 10 D. Nucci, C. Fatigoni, T. Salvatori, M. Nardi, S. Realdon and V. Gianfredi, *Int. J. Environ. Res. Public Health*, 2021, **18**, 4168.
- 11 S. Fuller, E. Beck, H. Salman and L. Tapsell, *Plant Foods Hum. Nutr.*, 2016, **71**, 1–12.
- 12 M. M. Ma and T. H. Mu, *Food Chem.*, 2016, **194**, 237–246, DOI: [10.1016/j.foodchem.2015.07.095](https://doi.org/10.1016/j.foodchem.2015.07.095).
- 13 W. Tang, X. Lin, N. Walayat, J. Liu and P. Zhao, *Crit. Rev. Food Sci. Nutr.*, 2024, **64**, 7895–7915, DOI: [10.1080/10408398.2023.2193651](https://doi.org/10.1080/10408398.2023.2193651).
- 14 J. Xu, Y. Li, Y. Zhao, D. Wang and W. Wang, *J. Funct. Foods*, 2021, **80**, 104434.
- 15 F. T. Macagnan, L. R. dos Santos, B. S. Roberto, F. A. de Moura, M. Bizzani and L. P. da Silva, *Bioact. Carbohydr. Diet. Fibre*, 2015, **6**, 1–6, DOI: [10.1016/j.bcdf.2015.04.001](https://doi.org/10.1016/j.bcdf.2015.04.001).
- 16 H. Chutia, M. Sharma, M. J. Das and C. L. Mahanta, *Waste Biomass Valorization*, 2024, **15**, 2345–2359, DOI: [10.1007/s12649-023-02288-0](https://doi.org/10.1007/s12649-023-02288-0).
- 17 I. Nandi and M. Ghosh, *Bioact. Carbohydr. Diet. Fibre*, 2015, **5**, 129–136, DOI: [10.1016/j.bcdf.2015.03.001](https://doi.org/10.1016/j.bcdf.2015.03.001).
- 18 M. Moczowska, S. Karp, Y. Niu and M. A. Kurek, *Food Hydrocoll.*, 2019, **90**, 105–112, DOI: [10.1016/j.foodhyd.2018.12.018](https://doi.org/10.1016/j.foodhyd.2018.12.018).
- 19 V. V. Khanpit, S. P. Tajane and S. A. Mandavgane, *Biomass Convers. Biorefin.*, 2025, **15**, 1667–1686, DOI: [10.1007/s13399-021-01980-2](https://doi.org/10.1007/s13399-021-01980-2).
- 20 F. Zhang, W. Yi, J. Cao, K. He, Y. Liu and X. Bai, *Int. J. Food Sci. Technol.*, 2020, **55**, 1781–1791, DOI: [10.1111/ijfs.14465](https://doi.org/10.1111/ijfs.14465).
- 21 H. Chen, M. Xiong, T. Bai, D. Chen, Q. Zhang, D. Lin, Y. Liu, A. Liu, Z. Huang and W. Qin, *LWT*, 2021, **149**, 111816, DOI: [10.1016/j.lwt.2021.111816](https://doi.org/10.1016/j.lwt.2021.111816).
- 22 H. Siddiqui, Z. Sultan, O. Yousuf, M. Malik and K. Younis, *Bioact. Carbohydr. Diet. Fibre*, 2023, **30**, 100356, DOI: [10.1016/j.bcdf.2023.100356](https://doi.org/10.1016/j.bcdf.2023.100356).
- 23 I. L. Gil-López, J. A. Lois-Correa, M. E. Sánchez-Pardo, M. A. Domínguez-Crespo, A. M. Torres-Huerta, A. E. Rodríguez-Salazar and V. N. Orta-Guzmán, *Ind. Crops Prod.*, 2019, **135**, 159–169, DOI: [10.1016/j.indcrop.2019.04.042](https://doi.org/10.1016/j.indcrop.2019.04.042).
- 24 S. Wang, Y. Fang, Y. Xu, B. Zhu, J. Piao, L. Zhu, L. Yao, K. Liu, S. Wang, Q. Zhang, L. Qin and J. Wu, *J. Funct. Foods*, 2022, **93**, 105081.
- 25 R. Kaur, P. S. Panesar, B. Kaur and C. S. Riar, *J. Food Sci. Technol.*, 2024, **61**, 1536–1546, DOI: [10.1007/s13197-023-05921-x](https://doi.org/10.1007/s13197-023-05921-x).
- 26 Y. Rammohan, T. Shuprajhaa, P. S. Kumar, V. Vasudevan, M. Sivaprasad, T. N. V. K. V. Prasad, V. N. P. S. Krishna and Y. Sireesha, *Int. J. Biol. Macromol.*, 2025, **311**, 143881, DOI: [10.1016/j.ijbiomac.2025.143881](https://doi.org/10.1016/j.ijbiomac.2025.143881).



- 27 P. S. Kumar, M. K. Birundha, S. Pushpavalli, R. Arthee, T. Shuprajhaa and G. C. Wakchaure, *Discover Food*, 2025, **5**, 231, DOI: [10.1007/s44187-025-00544-x](https://doi.org/10.1007/s44187-025-00544-x).
- 28 L. Wen, Z. Zhang, M. Zhao, R. Senthamaraiannan, R. B. Padamati, D.-W. Sun and B. K. Tiwari, *Int. J. Food Sci. Technol.*, 2020, **55**, 2242–2250, DOI: [10.1111/ijfs.14477](https://doi.org/10.1111/ijfs.14477).
- 29 L. K. Rawat and T. Ghosh, *Sustain. Food Technol.*, 2025, **3**, 204–214, DOI: [10.1039/D4FB00230J](https://doi.org/10.1039/D4FB00230J).
- 30 Association of Official Analytical Chemists, *Official Methods of Analysis*, AOAC International, Gaithersburg, MD, USA, 21st edn, 2019.
- 31 P. S. Kumar, S. Pushpavalli, D. A. Keran, T. Shuprajhaa, C. Sivananth, R. Renganathan, J. K. Jayaraman, P. Balakrishnan and S. Uma, *Food Chem.*, 2022, **397**, 133828, DOI: [10.1016/j.foodchem.2022.133828](https://doi.org/10.1016/j.foodchem.2022.133828).
- 32 S. Chinnathambi, P. S. Kumar, T. Shuprajhaa, K. N. Shiva and S. Narayanan, *Int. J. Biol. Macromol.*, 2024, **258**, 128989, DOI: [10.1016/j.ijbiomac.2023.128989](https://doi.org/10.1016/j.ijbiomac.2023.128989).
- 33 J. Gan, Z. Huang, Q. Yu, G. Peng, Y. Chen, J. Xie, S. Nie and M. Xie, *Food Hydrocoll.*, 2020, **101**, 105549, DOI: [10.1016/j.foodhyd.2019.105549](https://doi.org/10.1016/j.foodhyd.2019.105549).
- 34 F. Peng, X. Ren, B. Du, L. Chen, Z. Yu and Y. Yang, *Foods*, 2022, 2161.
- 35 Y. He, W. Li, X. Zhang, T. Li, D. Ren and J. Lu, *J. Food Sci. Technol.*, 2020, **57**, 1421–1429, DOI: [10.1007/s13197-019-04177-8](https://doi.org/10.1007/s13197-019-04177-8).
- 36 S. Chemat, A. Aissa, A. Boumechhour, O. Arous and H. Ait-Amar, *Ultrason. Sonochem.*, 2017, **34**, 310–316, DOI: [10.1016/j.ultsonch.2016.05.046](https://doi.org/10.1016/j.ultsonch.2016.05.046).
- 37 W. Routray, V. Orsat and Y. Gariepy, *Dry. Technol.*, 2014, **32**, 1888–1904.
- 38 C. Jiang, X. Zeng, X. Wei, X. Liu, J. Wang and X. Zheng, *Ultrason. Sonochem.*, 2024, **104**, 106817, DOI: [10.1016/j.ultsonch.2024.106817](https://doi.org/10.1016/j.ultsonch.2024.106817).
- 39 Z. Hassan, M. Imran, M. H. Ahmad and M. K. Khan, *J. Food Qual.*, 2021, **2021**, 5035299, DOI: [10.1155/2021/5035299](https://doi.org/10.1155/2021/5035299).
- 40 M. S. Ibrahim, M. Nadeem, M. Sultan, U. Sajjad, K. Hamid, T. M. Qureshi and S. Javaria, *Future Foods*, 2024, **9**, 100349, DOI: [10.1016/j.fufo.2024.100349](https://doi.org/10.1016/j.fufo.2024.100349).
- 41 Z. Yin, Z. Wang, Z. He, M. Zeng, F. Qin and J. Chen, *Food Biosci.*, 2021, **41**, 100898.
- 42 X. Yu, K. Zhu, F. Hu, R. Hu and W. Dong, *Ultrason. Sonochem.*, 2025, **114**, 107247.
- 43 Y. Gao, W. Xia, P. Shao, W. Wu, H. Chen, X. Fang, H. Mu, J. Xiao and H. Gao, *Curr. Opin. Food Sci.*, 2022, **48**, 100915, DOI: [10.1016/j.cofs.2022.100915](https://doi.org/10.1016/j.cofs.2022.100915).
- 44 Q. Li, S. Yang, Y. Li, Y. Huang and J. Zhang, *LWT*, 2019, **111**, 534–540, DOI: [10.1016/j.lwt.2019.05.086](https://doi.org/10.1016/j.lwt.2019.05.086).
- 45 J. Chu, H. Zhao, Z. Lu, F. Lu, X. Bie and C. Zhang, *Food Chem.*, 2019, **294**, 79–86, DOI: [10.1016/j.foodchem.2019.05.035](https://doi.org/10.1016/j.foodchem.2019.05.035).
- 46 M. Jia, J. Chen, X. Liu, M. Xie, S. Nie, Y. Chen, J. Xie and Q. Yu, *Food Hydrocoll.*, 2019, **94**, 468–474, DOI: [10.1016/j.foodhyd.2019.03.047](https://doi.org/10.1016/j.foodhyd.2019.03.047).
- 47 T. Liu, H. Lei, X. Zhen, J. Liu, W. Xie, Q. Tang, D. Gou and J. Zhao, *Food Chem.*, 2024, **458**, 140154, DOI: [10.1016/j.foodchem.2024.140154](https://doi.org/10.1016/j.foodchem.2024.140154).
- 48 X. Li, B. Wang, W. Hu, H. Chen, Z. Sheng, B. Yang and L. Yu, *Food Chem. X*, 2022, **14**, 100274.
- 49 H. Sun, W. Ge, D. Song, Y. Li, Y. Wang and H. Wang, *Food Biosci.*, 2024, **61**, 104703.
- 50 B. Chen, X. Liu, X. Guo, L. Tang, G. Su, Z. Lin, J. Sun, B. Wang, L. Tao and F. Wang, *Food Chem.*, 2025, **496**, 146821, DOI: [10.1016/j.foodchem.2025.146821](https://doi.org/10.1016/j.foodchem.2025.146821).

